Progress In Electromagnetics Research M, Vol. 35, 21–30, 2014

Substrate Integrated Waveguide Design Using the Two Dimentionnal Finite Element Method

Mohammed A. Rabah[1], Mehadji Abri[1, *], Jun Wu Tao[2], and Tan-Hoa Vuong[2]

Abstract—In this paper, a rigorous and accurate numerical two-dimensional modeling finite element method 2D-FEM is applied to the analysis and design of substrate integrated waveguide components. The finite element method represents an excellent tool for the analysis and design since it easily allows taking into account all details of each device. The advantages of this method have been proved with the successful design of two SIW waveguide topologies operating in [8–12] GHz and [10.7–12.75] GHz respectively for X-band and Ku-band applications employed in satellite communications. In order to validate the proposed method, a comparison is made between the FEM method implemented in Matlab and CST Microwave Studio® software. Agreements between the finite element method data and the CST software results were achieved. The obtained results show the effectiveness of this method to analyze such types of guides.

1. INTRODUCTION

Waveguide is a traditional transmission line employed for microwave signal guidance and processing, and it is still widely used today for many applications. Various microwave waveguide components, such as couplers, detectors, isolators, phase shifters and slotted lines, are commercially available for various standard waveguide bands. It is also known that these matured waveguide components present properties of low loss and high power.

Because of their bulky size, their use is however limited in some of practical applications, and it is also difficult to manufacture them in mass production. With trends toward miniaturization and integration, planar transmission line structures, such as microstrip and stripline rather than waveguide, have been used in many commercial applications. There is, however, still a huge demand for waveguides in loss- and/or power-sensitive applications. Therefore, it would be much meaningful for microwave applications if we can combine the advantages of planar transmission lines with those of waveguides. There have been many research activities to develop new platforms of transmission lines to reduce circuit size, simplify manufacture process, lower production cost and maintain high performance. To overcome these issues, substrate integrated waveguides (SIW) have recently been proposed [1–7] as alternative structures to conventional transmission lines. Substrate integrated waveguides are synthetic rectangular waveguides formed by top and bottom metal layers which embed a dielectric slab and two sidewalls of metallic vias and it can be easily fabricated with standard PCB process, thick-film process or LTCC process, and is easily integrated into microwave and millimeter wave integrated circuits. This technology is one of the most popular and the most developed platforms.

Due to the advantages of this new technology, it is convenient to develop numerical methods for the accurate and efficient simulation of such components. To analyze this type of guides, rigorous numerical methods are needed. Several methods are available and proposed in literature [8–17].

Received 7 January 2014, Accepted 7 February 2014, Scheduled 15 February 2014

* Corresponding author: Mehadji Abri (abrim2002@yahoo.fr).

[1] Laboratoire de Télécommunications, Département de Génie Electrique, Faculté de Technologie, Université Abou-Bekr Belkaïd, Tlemcen, BP 230, Pôle Chetouane, Tlemcen 13000, Algeria. [2] Laboratoire de Laplace, Université de Toulouse, France.

Currently the FEM finite element method has a fundamental role in the analysis of various problems related to electromagnetism, from a simple structure as a waveguide to complex circuits and antennas. The FEM remains the most common method used by CAD softwares. Advantages of this method come from its ability to analyze complex geometries.

The finite element method implemented in the MATLAB® software is applied for analysis and design of SIW waveguides operating in X and Ku-band applications. The implementation of the finite element methods is not easy because it requires tedious and complex analytical formulation development before going to the implementation.

This paper is organized as follows: in Section 2, the finite element method modal expansion formulation is presented. Section 3 presents the FEM Implementations. Section 4 describes the geometry and design rules. The obtained results and the comparison made between the FEM and the CST Microwave Studio software are reported in Section 5. Finally, conclusions are drawn in Section 6.

2. THE FINITE ELEMENT MODAL EXPANSION FORMULATION

Let us assume that the junction is excited with the fundamental mode TE_{10} through its ports. The finite element formulation of the problem will be carried out considering the case of an H-plane junction. The top view of the geometry as well as the reference systems used for the analysis of a generic H-plane junction are shown in Figure 1. The finite element method is applied in the region Ω and is delimited by a perfectly conducting wall Γ_0 and by two defined ports Γ_k ($k = 1, 2$). The electric field into the region Ω has the only component E_y.

The components of the electric and magnetic fields, $E_{y_{wg}}$ and $H_{x_{wg}}$, when the port j is fed with the TE_{10} mode can be expressed as [18]:

$$E_{y_{wg}}(x) = \delta_{kj} e_1^j \left(x^j\right) e^{j\beta_1^j z^j} + \sum_{m=1}^{\infty} B_m^k e_m^k \left(x^k\right) e^{-j\beta_m^k z^k} \tag{1}$$

$$j\omega\mu_0 H_{x_{wg}}(x) = \frac{\partial E_{y_{wg}}}{\partial z} \tag{2}$$

where e_1 is the orthonormal modal functions of the TE_{10} mode.

$$e_1(x) = \frac{2}{\sqrt{ab}} \sqrt{\frac{k_0 Z_0}{\beta_1}} \sin\left(\frac{m\pi}{a} x\right) \tag{3}$$

k_0 and Z_0 are the free-space propagation constant and characteristic impedance, respectively. β_1 denotes the propagation constant into the waveguide with dimensions a and b:

$$\begin{cases} \beta_1 = \sqrt{k_0^2 - k_c^2} & \text{for } k_0^2 \geq k_c^2 \\ \beta_1 = -j\sqrt{k_c^2 - k_0^2} & \text{for } k_c^2 > k_0^2 \end{cases} \tag{4}$$

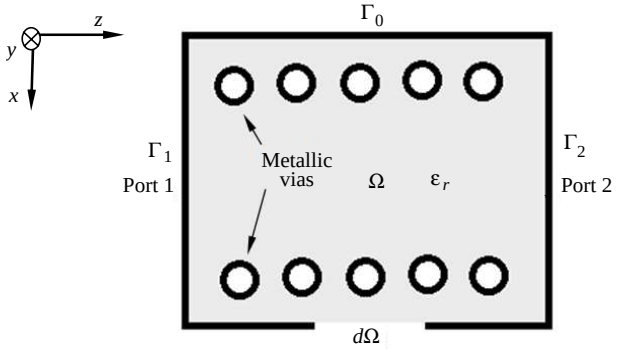

Figure 1. Structure under study in H-plane. The domain Ω is embedded in a rectangle with contour $d\Omega$.

and $k_c = \frac{m\pi}{a}$ is the cutoff propagation constant of mode TE_{10}.

Inside the inhomogeneous region Ω, the field cannot be expressed in terms of analytically known functions, thus the problem is solved seeking the solution of the scalar Helmholtz equation:

$$\nabla_t \left(\frac{1}{\mu_r} \nabla_t E_y \right) + k_0^2 \varepsilon_r E_y = 0 \tag{5}$$

where: ε_r and μ_r are respectively the relative permittivity and permeability.

The homogeneous boundary conditions are:

$$E_y{=}0, \quad k = 1, 2 \tag{6}$$

At the metallic wall Γ_0:

$$E_y|_{\Gamma_k} = E^k_{y_{wg}}, \quad k = 1, 2 \tag{7}$$

$$H_x|_{\Gamma_k} {=} H^k_{x_{wg}}, \quad k = 1, 2 \tag{8}$$

$$\left.\frac{\partial E_y}{\partial n}\right|_{\Gamma_k} {=} \frac{\partial E^k{}_{y_{wg}}}{\partial z}, \quad k = 1, 2 \tag{9}$$

By using the weighted residual procedure, by choosing arbitrary differentiable weighting functions W, $\bar{W}$, and $\bar{\bar{W}}$, (5), (6), (7) and (9) can be replaced by:

$$\iint_\Omega W \nabla_t \cdot \left(\frac{1}{\mu} \nabla_t E_y \right) d\Omega + \iint_\Omega k_0^2 \varepsilon_r W E_y d\Omega = 0 \tag{10}$$

$$\int_{\Gamma_0} \bar{W} E_y d\Gamma_0 = 0 \tag{11}$$

$$\int_{\Gamma_k} \bar{W} E_y d\Gamma_k = \int_{\Gamma_k} \bar{W} E^k{}_{y_{wg}} d\Gamma_k, \quad k = 1, 2 \tag{12}$$

$$\int_{\Gamma_k} \bar{\bar{W}} \frac{\partial E_y}{\partial n} d\Gamma_k = \int_{\Gamma_k} \bar{\bar{W}} \frac{\partial E^k_{y_{wg}}}{\partial z} d\Gamma_k, \quad k = 1, 2 \tag{13}$$

By applying Green's identity to (10) and introducing the boundary condition (13), leads to the weak form of the Helmholtz equation:

$$\iint_\Omega W \nabla_t \cdot \left(\frac{1}{\mu} \nabla_t E_y \right) d\Omega {-} k_0^2 \iint_\Omega \varepsilon_r W E_y d\Omega - \int_{\Gamma_k} W \frac{\partial E^k_{y_{wg}}}{\partial z^k} d\Gamma_k = 0 \tag{14}$$

3. THE FINITE ELEMENT IMPLEMENTATION

The solution (12) and (14) for H-plane junction using finite elements in the framework of the weighted residual procedure is based on the following five steps:

- The region of guide is divided into finite elements;
- Simplify the unknown function on each element;
- Giving weighting functions and express the residue on each element;
- Summing up contributions from all elements to obtain the residue on the whole domain;
- Annihilating the residue and solve the linear system of equations obtained.

The solution on each element (e) is required among the approximating functions $\bar{E}_y^{(e)}$ of the form:

$$\bar{E}_y^{(e)}(x, y) = \sum\nolimits_{j=1}^{N^{(e)}} \bar{E}_{y_j}^{(e)} \alpha_j^{(e)}(x, y) \tag{15}$$

where: $\bar{E}_{y_j}^{(e)}$ and $\alpha_j^{(e)}$ (x, y) $(j = 1 \ldots N^{(e)})$ are the coefficients and the set of nodal-shape functions, respectively. $W_i^{(e)}$ presented in Figure 2 are the weighting functions equal to the shape functions, $W_i^{(e)} = \alpha_i^{(e)}$ $(i = 1 \ldots N^{(e)})$.

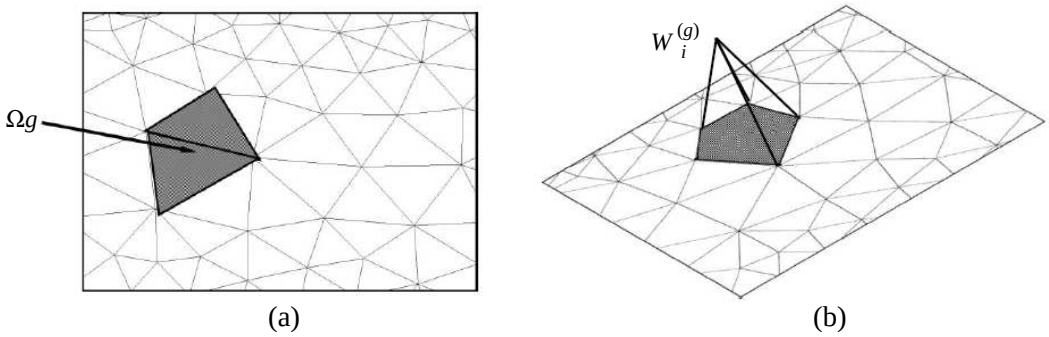

Figure 2. Global weighting function $W_i^{(g)}$ obtained by connecting first-order weighting functions defined on adjacent elements and centered at the same global node i.

$R_i^{(e)}$ is the residue relative to the ith weighting function, with:

$$\frac{1}{\mu_r}\iint_{\Delta^{(e)}} \nabla_t \alpha_i^{(e)} \cdot \nabla_t \bar{E}_y^{(e)} d\Omega - k_0^2 \epsilon_r \iint_{\Delta^{(e)}} \alpha_i^{(e)} \bar{E}_y^{(e)} d\Omega - \sum\nolimits_{k=1}^{N} \int_{\Gamma_k^{(e)}} \alpha_i^{(e)} \frac{\partial E_{y_{wg}}^{(k)}}{\partial z^{(k)}} d\Gamma_k = 0 \tag{16}$$

Alternatively, in matrix form:

$$\frac{1}{\mu_r}\left[S^{(e)}\right] \cdot \left[\bar{E}_y^{(e)}\right] - k_0^2 \epsilon_r \left[T^{(e)}\right] \cdot \left[\bar{E}_y^{(e)}\right] + \sum\nolimits_{k=1}^{N} \left\{\left[C_k^{(e)}\right] \cdot [B_k] - \left[H_k^{(e)}\right]\right\} = \left[R^{(e)}\right] \tag{17}$$

where:

- $[S^{(e)}]$ and $[T^{(e)}]$ present the usual local matrices of scalar nodal element.
- $[\bar{E}_y^{(e)}]$ is the vector of nodal unknown coefficients of element (e).
- $[B_k]$ is a column vector, whose jth entry is the amplitude of the transmitted mode j at the port k.
- $[C_k^{(e)}]$ and $[H_k^{(e)}]$ come from the contour integrals at the $k = 1 \ldots N$ ports.

$[C_k^{(e)}]$ and $[H_k^{(e)}]$ are given by:

$$C_{k_{im}}^{(e)} = j\beta_m^{(k)} \int_{\Gamma_k^{(e)}} \alpha_i^{(e)} e_m^{(k)} d\Gamma_k^{(e)} = j\beta_m^{(k)} \frac{2}{\sqrt{a^{(k)} b}} \sqrt{\frac{k_0 Z_0}{\beta_m^{(k)}}} \int_{\Gamma_k^{(e)}} \alpha_i^{(e)} \sin\left(\frac{m\pi}{a^{(k)}} x^{(k)}\right) d\Gamma_k^{(e)} \tag{18}$$

$$H_{k_i}^{(e)} = j\beta_1^{(l)} \delta_{kl} \int_{\Gamma_k^{(e)}} \alpha_i^{(e)} e_1^{(l)} d\Gamma_k^{(e)} = \delta_{kl} j\beta_1^{(l)} \frac{2}{\sqrt{a^{(l)} b}} \sqrt{\frac{k_0 Z_0}{\beta_1^{(l)}}} \int_{\Gamma_k^{(e)}} \alpha_i^{(e)} \sin\left(\frac{\pi}{a^{(l)}} x^{(l)}\right) d\Gamma_k^{(e)} \tag{19}$$

where, (l) is the port fed and δ_{kl} is the Kronecker's delta.

The local residual (17) relative to each element can be assembled into a single linear system of equations, where the matrix $[F]$ assembles the two matrices $[S^{(e)}]$ and $[T^{(e)}]$ with a dimension of $(N_n \times N_n)$, $[F]$, with N_n total number of nodes. The matrix $[C]$ assembles the matrix $[C_k^{(e)}]$ and the vector $[H_k^{(e)}]$ with a dimension of $(N_n \times (N \times M))$. The matrix $[H^{inc}]$ presented by the column $(N \times 1)$.

For both entities, the assembling approach to recover the row index in the global matrix/vector is the same as that used for the local matrices $[S^{(e)}]$ and $[T^{(e)}]$. The assembling scheme for the column index j of matrix $[C]$ is readily determined by the formula $j = M \times (k-1) + m$, which means that the unknown amplitudes of transmitted modes at different ports are sequentially arranged in a unique column vector $[B]$ with dimension $((N \times M) \times 1)$. Annihilating the residue of the assembled system leads to the matrix equation [18]:

$$[F] \cdot \left[\bar{E}\right] + [C] \cdot [B] = \left[H^{inc}\right] \tag{20}$$

In this formula, the unknowns are the column vectors $[\bar{E}]$ and $[B]$.

The matrix $[\bar{E}]$ contains the coefficients of the finite element approximation of the electric field, and $[B]$ stores the amplitude of the transmitted field at the ports. To construct these equations, the boundary condition (12) is used. A particularly convenient choice for the basic functions $\bar{W}_m^{(k)}$, $m = 1 \ldots M$ to be used at port (k) is:

$$\bar{W}_m^{(k)} = \sin\left(\frac{m\pi}{a^{(k)}} x^{(k)}\right) \tag{21}$$

Using these weighting functions, the residue $R_m^{(k)}$ of the boundary condition (12) relative to the m-th weighting function at port (k) is expressed as:

$$\int_{\Gamma_k} \sin\left(\frac{m\pi}{a^{(k)}} x^{(k)}\right) \bar{E}_y d\Gamma_k - \sqrt{\frac{a^{(k)}}{b}} \sqrt{\frac{k_0 Z_0}{\beta_m^{(k)}}} B_m^{(k)} - \delta_{kl} \sqrt{\frac{a^{(l)}}{b}} \sqrt{\frac{k_0 Z_0}{\beta_1^{(l)}}} = R_m^{(k)}, \quad m = 1 \ldots M \tag{22}$$

The above equation, relative to port (k), can be made from the matrix:

$$[D_k] \cdot \left[\bar{E}_y^{(k)}\right] + [A_k] \cdot [B_k] - [E_k] = \left[R^k\right] \tag{23}$$

where the column vector $[\bar{E}_y^{(k)}]$ $(N^{(k)} \times 1)$ stores the finite element coefficients of the electric field associated to the $N^{(k)}$ nodes at port (k). $[D_k]$ is a rectangular matrix $(M \times N^{(k)})$ with generic entry $D_{k_{mj}}$:

$$D_{k_{mj}} = \int_{\Gamma_k} \sin\left(\frac{m\pi}{a^{(k)}} x^{(k)}\right) \alpha_j^{(k)} d\Gamma_k \tag{24}$$

The matrix $[A_k]$ is diagonal with entries:

$$A_{k_{mm}} = -\sqrt{\frac{a^{(k)}}{b}} \sqrt{\frac{k_0 Z_0}{\beta_m^{(k)}}} \quad m = 1 \ldots M \tag{25}$$

The column vector $[E_k]$ $(M \times 1)$ takes into account the incident field, if any, at port (k). It has only one nonzero entry that is pertinent to the fundamental TE_{10} mode:

$$E_{k_1 = \delta_{kl}} \sqrt{\frac{a^{(l)}}{b}} \sqrt{\frac{k_0 Z_0}{\beta_1^{(l)}}} E_{k_m} = 0 \quad m = 2 \ldots M \tag{26}$$

The continuity boundary conditions at each port, expressed by (23), can be assembled into a global system and the residue annihilated. Combining such a system with that in (20) eventually yields the total system of equations to be solved, which has the structure:

$$\begin{bmatrix} [A] & [D] \\ [C] & [F] \end{bmatrix} \cdot \begin{bmatrix} [B] \\ [E] \end{bmatrix} = \begin{bmatrix} [E^{inc}] \\ [H^{inc}] \end{bmatrix} \tag{27}$$

4. GEOMETRY AND DESIGN RULES

The SIW waveguide is filled with a dielectric, so we can use the formulas to design a classical waveguide to reconstruct the geometric parameters of a substrate integrated waveguide. For the TE_{10} mode, the simplified version of this formula is:

$$f_c = \frac{c}{2a} \tag{28}$$

For a filled waveguide (FW) as shown in Figure 3, with same cut off frequency, dimension "a_{FW}" is found by:

$$a_{\mathrm{FW}} = \frac{a}{\sqrt{\varepsilon_r}} \tag{29}$$

Having determined the dimension "a_{FW}" for the filled waveguide, we can now pass to the design equations for SIW [19].

$$a_s = a_{\mathrm{FW}} + \frac{d^2}{0.95s} \tag{30}$$

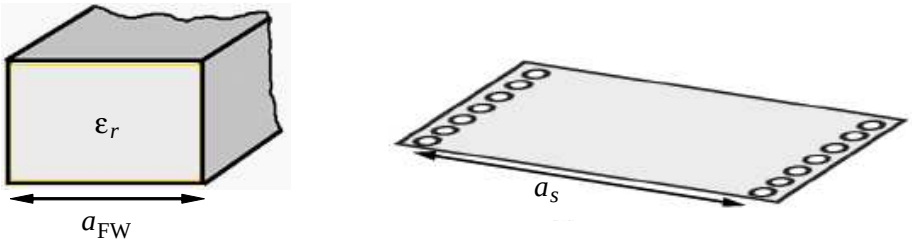

Figure 3. Dimensions for: (a) FW, (b) SIW.

where d is via diameter and s is the distance between the vias.

For SIW design, the following two conditions are required:

$$d < \frac{\lambda_g}{5} \tag{31a}$$

$$s \leq 2d \tag{31b}$$

λ_g is the guided wavelength:

$$\lambda_g = \frac{2\pi}{\sqrt{\frac{(2\pi f)^2 \varepsilon_r}{c^2} - \left(\frac{\pi}{a}\right)^2}} \tag{32}$$

Our goal is to produce a SIW waveguide with best transmission, because we must adapt our structure. A transition from a microstrip line to the waveguide SIW is necessary. The formula used to calculate the waveguide impedance of the SIW is given by:

$$Z_{pi} = Z_{\mathrm{TE}} \frac{\pi^2 h}{8 a_s} \tag{33}$$

For the calculation of the guide impedance, it is also necessary to calculate the wave impedance of TE mode, which is given by:

$$Z_{\mathrm{TE}} = j\omega \frac{\mu}{\gamma} = \omega \frac{\acute{\mu}}{\beta} = \sqrt{\frac{\mu}{\varepsilon}} \times \frac{\lambda_g}{\lambda} \tag{34}$$

5. SIMULATION RESULTS

2D-FEM analysis of such a problem becomes more efficient once it is recognized that, for posts with a constant section that extends the whole height of the substrate integrated waveguide, a TE_{10} excitation will produce only $\mathrm{TE}_{\mathrm{m0}}$ modes and that the three-dimensional problem can be reduced to a two-dimensional one by analyzing only the E_y field component on an H plane cut [20]. Figure 4(b) shows a mesh of such cut. The analysis is done on the entire SIW waveguide with a perfect electric conductor (p.e.c) boundary.

The first task of the analysis is building the geometric model and its finite element discretization using the mesh generator. Figures 5 and 6 show an analysis of 15 and 26 equally spaced via-hole pairs respectively for X and Ku bands with microstrip input and all-dielectric waveguide output.

The first test case is a simple SIW waveguide enclosed by p.e.c. walls, with dimensions as shown in Figure 7 and Figure 8 for X and Ku bands, respectively.

The SIW waveguide considered for this investigation is is to be designed on Arlon Cu 233LX lossy substrate which has a relative permittivity ε_r of 2.2, a dielectric thickness h of 0.508 mm, a loss tangent of about 0.0013 and 0.05 mm conductor thickness. The SIW waveguide is designed to operate over the frequency range [8–12 GHz] and [10.7–12.75 GHz] respectively for X-band and Ku-band applications. Because the input impedance of the SIW waveguide at its edges is usually too high for direct connection to the feeding line, whose standard impedance is 50 Ohm. SIW guide adaptation is necessary; in this case, a microstrip transition can be designed to achieve a satisfactory return loss at the operating band frequency.

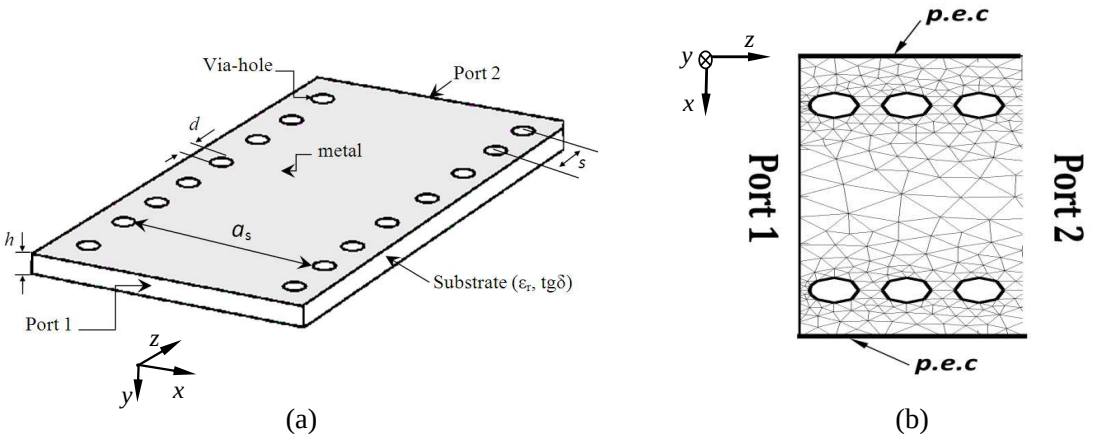

Figure 4. (a) SIW waveguide in dielectric. (b) Two-dimensional mesh of the full domain with p.e.c. wall.

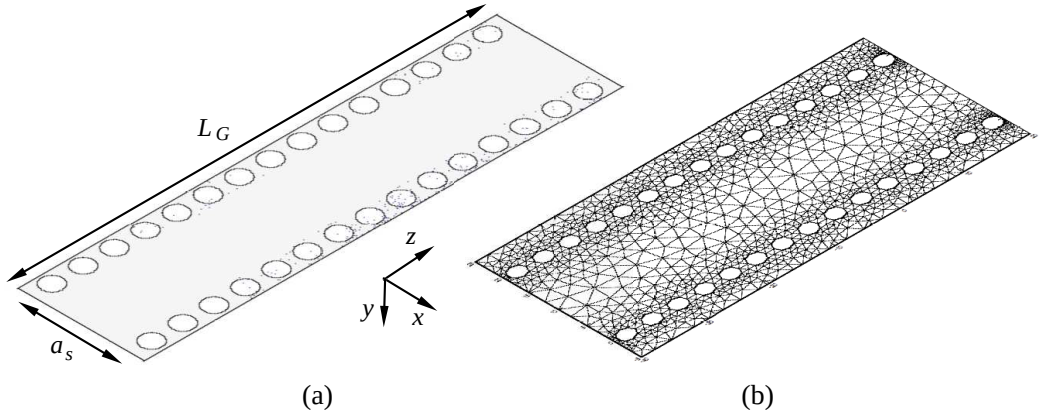

Figure 5. (a) X-band SIW waveguide. (b) Mesh of SIW guide operates in the X-band generated by the finite element method.

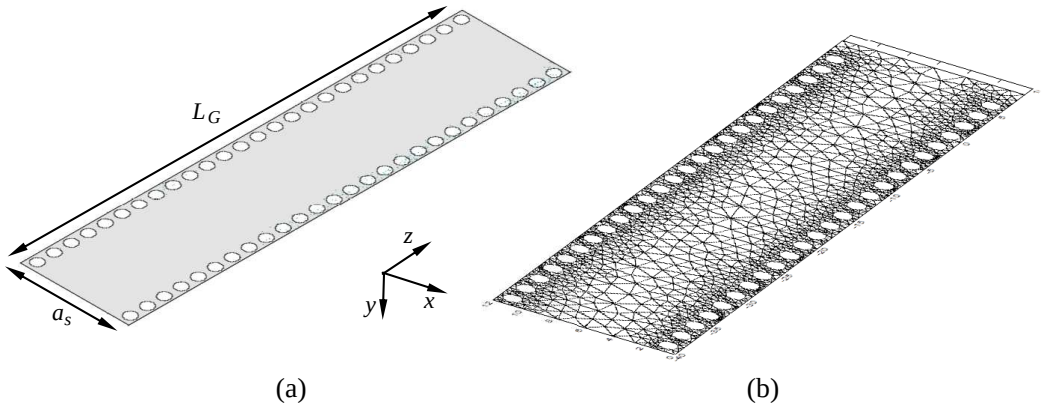

Figure 6. (a) Ku-band SIW waveguide. (b) Mesh structure generated by the finite element method in the Ku-band.

Figures 7 and 8 depict respectively the optimized proposed configuration of the X and Ku-band waveguides based on SIW with their physical parameters. 50 Ohm microstrip transitions from 50 Ohm to the waveguides impedance are used in input and output.

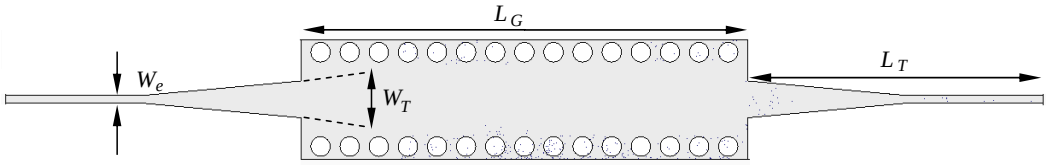

Figure 7. X band SIW waveguide. The parameters of this waveguide defined by: $W_e = 1.3\,\text{mm}$, $W_T = 6.16\,\text{mm}$, $L_T = 50.14\,\text{mm}$, $a_s = 17.73\,\text{mm}$, $d = 3.30\,\text{mm}$, $s = 4.95\,\text{mm}$, $L_G = 76\,\text{mm}$.

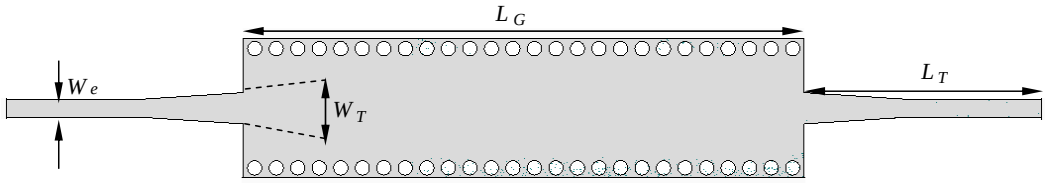

Figure 8. Ku band SIW waveguide. The parameters of this waveguide defined by: $a_s = 10.32\,\text{mm}$, $d = 1.25\,\text{mm}$, $s = 1.88\,\text{mm}$, $W_e = 1.59\,\text{mm}$, $W_T = 2.71\,\text{mm}$, $L_T = 20.72\,\text{mm}$, $L_G = 49\,\text{mm}$.

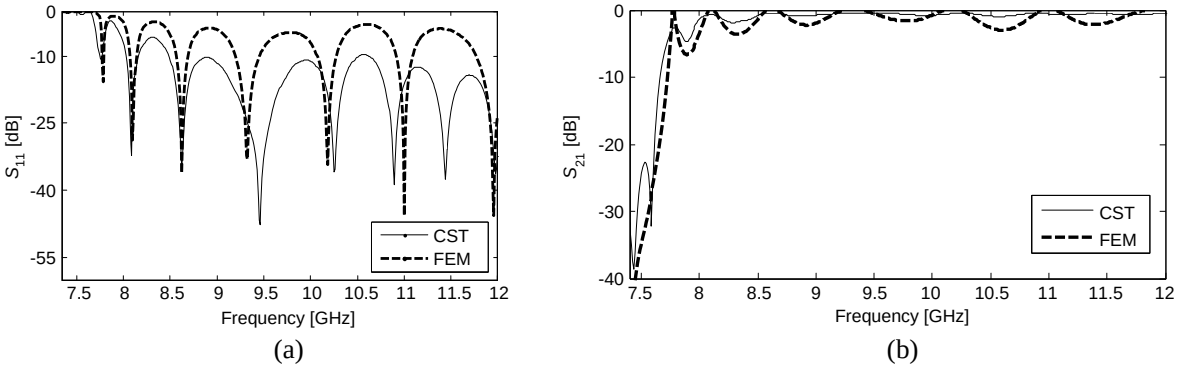

Figure 9. X-band return loss and transmission coefficient.

Since the two-dimensional finite element method simulates only the SIW waveguide without the transition, the later can be simulated with any software, and the obtained result is stored in a matrix $[S_T]$. The final matrix can be calculated by the following expression.

$$\begin{bmatrix} S_{11} & S_{12} \\ S_{21} & S_{22} \end{bmatrix} = [S_T]\,[S_{\text{siw}}]\,[S_T] \tag{35}$$

Figures 9 and 10 display a comparison between the finite element method and the CST Softaware for X and Ku-band respectively.

Let us notice from Figures 9(a) and 10(a) that below the cutoff frequencies respectively $f_c = 7.75\,\text{GHz}$ for the X-band waveguide and $f_c = 10.70\,\text{GHz}$ for the Ku-band waveguide, the return loss is maximal, about 0 dB. The corresponding transmission is minimal as shown in Figures 9(b) and 10(b). It can be observed that a good rejection is obtained from the provided results.

The simulations was performed using an Intel (R) Core (TM), i7-2600 CPU@3.40 GHz with 8 Go RAM memory on the same computer, without simulation parallelization and hardware acceleration. It was observed that FEM method running time is the half of the CST one.

Beyond range frequency [7.75–12 GHz] for the X-band waveguide and [10.70–12.60 GHz] for the Ku-band, the transmission is significantly improved. Several resonance peaks are found with levels less than −20 dB. Let us notice that the comparison made between the two-dimensional finite element method and CST gives good results. A major observation in Figure 9 is that the two graphs are almost identical, and a good agreement is observed between this two approaches. Some differences are observed

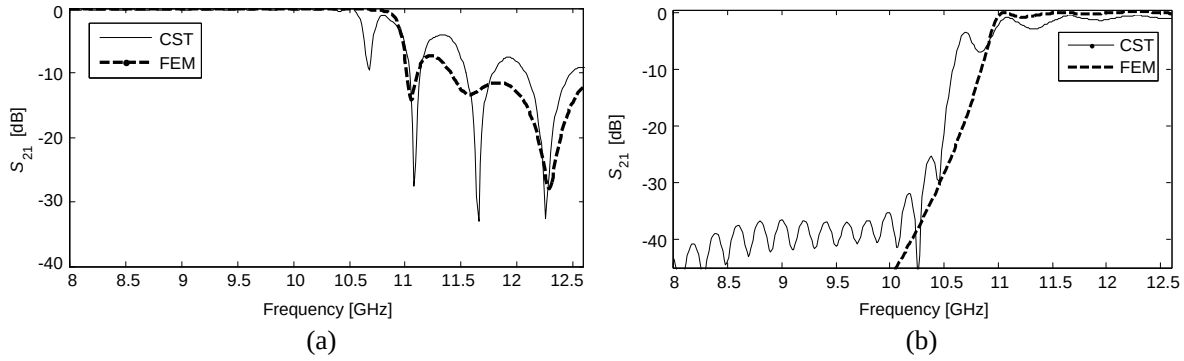

Figure 10. Ku-band return loss and transmission coefficient.

in the return loss performance. However, the shifts are small and occur in the return loss level. The comparison results show the effectiveness of the two-dimensional finite element method in studying the SIW waveguide performances.

6. CONCLUSION

A rigorous analytical full-wave analysis method for the precise modelling of SIW structures is proposed in this paper. The efficiency of the method has been shown through the analysis and design of two SIW waveguides operating in X and Ku bands. Even the implementation of the finite element method used to solve a series of formula to decompose a problem in finite element is too hard; it offers a good accuracy compared with other full wave methods. The exploitation of finite element method in electromagnetic field offers another vision of applying this method to examine and study other components based on the substrate integrated waveguides technology such as filters, couplers, etc.

ACKNOWLEDGMENT

The authors wish to acknowledge support for this work from the laboratory of Laplace of University of Toulouse-France would like to express his sincere thanks to Prof. J. W. Tao for his help.

REFERENCES

1. Wu, K., D. Deslandes, and Y. Cassivi, "The substrate integrated circuits — A new concept for high-frequency Electronics and Optoeletronics," *6th International Conference on Telecommunications in Modern Satellite, Cable and Broadcasting Service, TELSIKS 2003*, Vol. 1, P-III–P-X, Oct. 2003.
2. Kazemi, R., R. A. Sadeghzadeh, and A. E. Fathy, "Design of a wide band eight-way compact SIW power combiner FED by a low loss GCPW-to-SIW transition," *Progress In Electromagnetics Research C*, Vol. 26, 97–110, 2012.
3. Cassivi, Y., L. Perregrini, P. Arcioni, M. Bressan, K. Wu, and G. Conciauro, "Dispersion characteristics of substrate integrated rectangular waveguide," *IEEE Microwave Wireless Compon. Lett.*, Vol. 12, No. 9, 333–335, Sep. 2002.
4. Ruiz-Cruz, J. A., M. A. E. Sabbagh, K. A. Zaki, J. M. Rebollar, and Y. Zhang, "Canonical ridge waveguide filters in LTCC or metallic resonators," *IEEE Trans. Microw. Theory Tech.*, Vol. 53, No. 1, 174–182, Jan. 2005.
5. Chen, X.-P., K. Wu, and Z.-L. Li, "Dual-band and triple-band substrate integrated waveguide filters with Chebyshev and quasi-elliptic responses," *IEEE Trans. Microw. Theory Tech.*, Vol. 55, No. 12, 2569–2577, Dec. 2007.
6. Cassivi, Y. and K. Wu, "Low cost microwave oscillator using substrate integrated waveguide cavity," *IEEE Microwave Wireless Compon. Lett.*, Vol. 13, No. 2, 48–50, Feb. 2003.

7. Shen, W., W. Y. Yin, and X. W. Sun, "Miniaturized dual-band substrate integrated waveguide filter with controllable bandwidths," *IEEE Microwave Wireless Compon. Lett.*, Vol. 21, No. 8, 418–420, 2011.
8. Kanellopoulos, V. N. and J. P. Webb, "A complete E-plane analysis of waveguide junctions using the finite element method," *IEEE Trans. Microw. Theory Tech.*, Vol. 38, No. 3, 290–295, 1990.
9. Coccioli, R., R. Pelosi, and S. Selleri, "Optimization of bends in rectangular waveguide by a finite element-genetic algorithm procedure," *Microwave and Optical Technology Letters*, Vol. 16, No. 5, 287–290, Dec. 1997.
10. Sun, D.-K., L. Vardapetyan, and Z. Cendes, "Dimensional curl-conforming singular elements for FEM solutions of dielectric waveguide structures," *IEEE Trans. Microw. Theory Tech.*, Vol. 53, No. 3, 984–992, Mar. 2005.
11. Zeid, A. and H. Baudrand, "Electromagnetic scattering by metallic holes and its applications in microwave circuit design," *IEEE Trans. Microw. Theory Tech.*, Vol. 50, No. 4, 1198–1206, Apr. 2002.
12. Diaz Caballero, E., H. Esteban, A. Belenguer, and V. Boria, "Efficient analysis of substrate integrated waveguide devices using hybrid mode matching between cylindrical and guided modes," *IEEE Trans. Microw. Theory Tech.*, Vol. 60, No. 2, 232–243, Feb. 2012.
13. Wu, X. and A. Kishk, "Hybrid of method of moments and cylindrical eigenfunction expansion to study substrate integrated waveguide circuits," *IEEE Trans. Microw. Theory Tech.*, Vol. 56, No. 10, 2270–2276, Oct. 2008.
14. Arnieri, E. and G. Amendola, "Analysis of substrate integrated waveguide structures based on the parallel-plate waveguide Green's function," *IEEE Trans. Microw. Theory Tech.*, Vol. 56, No. 7, 1615–1623, 2008.
15. Abaei, E., E. Mehrshahi, G. Amendola, E. Arnieri, and A. Shamsafar, "Two dimensional multi-port method for analysis of propagation characteristics of substrate integrated waveguide," *Progress In Electromagnetics Research C*, Vol. 29, 261–273, 2012.
16. Bozzi, M., L. Perregrini, and K. Wu, "Modeling of losses in substrate integrated waveguide by boundary integral-resonant mode expansion method," *IEEE MTT-S International Microwave Symposium Digest*, 515–518, 2008.
17. Arnieri, E. and G. Amendola, "Method of moments analysis of slotted substrate integrated waveguide arrays," *IEEE Transactions on Antennas and Propagation*, Vol. 59, No. 4, 1148–1154, 2011.
18. Pelosi, G., R. Coccioli, and S. Selleri, *Quick Finite Elements for Electromagnetic Waves,* 2nd Edition, Artech House, Boston, 2009.
19. Doucha, S. and M. Abri, "New design of leaky wave antenna based on SIW technology for beam steering," *International Journal of Computer Networks & Communications (IJCNC)*, Vol. 5, No. 5, 73, Sep. 2013.
20. Fedi, G., S. Manetti, G. Pelosi, and S. Selleri, "FEM-trained artificial neural networks for the analysis and design of cylindrical posts in a rectangular waveguide," *Electromagnetics*, Vol. 22, No. 4, 323–330, 2002.

Errata to "Substrate Integrated Waveguide Design Using the Two Dimentionnal Finite Element Method"

by Mohammed A. Rabah, Mehadji Abri, Jun Wu Tao, and Tan-Hoa Vuong, in Progress In Electromagnetics Research M, Vol. 35, 21–30, 2014.

Mohammed A. Rabah[1], Mehadji Abri[1, *], Jun Wu Tao[2], and Tan-Hoa Vuong[2]

In page 28, the correct Equation (35) is:

$$\begin{bmatrix} T_{11} & T_{12} \\ T_{21} & T_{22} \end{bmatrix} = [T_T][T_{SIW}][T_T] \tag{35}$$

where:

$$\begin{bmatrix} b_1 \\ a_1 \end{bmatrix} = [T] \begin{bmatrix} a_2 \\ b_2 \end{bmatrix} \tag{36}$$

$$[S_T] = \begin{bmatrix} \dfrac{T_{12}}{T_{22}} & \dfrac{T_{11}T_{22} - T_{21}T_{12}}{T_{22}} \\ \dfrac{1}{T_{22}} & -\dfrac{T_{21}}{T_{22}} \end{bmatrix} \tag{37}$$

Received 25 June 2016, Added 29 June 2016

* Corresponding author: Mehadji Abri (abrim2002@yahoo.fr).

[1] Laboratoire de Télécommunications, Département de Génie Electrique, Faculté de Technologie, Université Abou-Bekr Belkaïd, Tlemcen, BP 230, Pôle Chetouane, Tlemcen 13000, Algeria. [2] Laboratoire de Laplace, Université de Toulouse, France.